JOURNAL OF APPLIED ELECTROCHEMISTRY 17 (1987) 724–730

Recirculating feed operation of bipolar packed-bed and trickle-bed electrode cells equipped with mesh spacers

KATSUKI KUSAKABE, TAKESHI KIMURA, SHIGEHARU MOROOKA, YASUO KATO

Department of Applied Chemistry, Kyushu University, Higashi-ku, Fukuoka, 812 Japan

Received 23 June 1986; revised 3 October 1986

Unsteady state changes in ion concentration, liquid conductivity and electric current via different pathways in a bipolar packed-bed electrode cell were investigated by using the electrochemical reduction of Cu(II) ions. Ferrite pellets were used as particle electrodes and were packed in layers separated by plastic spacers. The electrode reaction rate was controlled by the diffusion of Cu(II) ions.

The faradaic current passing through the pellets decreased with time, while the bypass current through the liquid bulk phase increased with time because of the production of hydrogen ions. The faradaic and bypass currents and the overall current efficiency were well simulated by a proposed reactor model.

The overall current efficiency unavoidably decreased with time when the electrolyte was recirculated. However, the employment of trickle flow reduced the liquid hold-up in the bed and consequently reduced the bypass current. The overall current efficiency in the trickle-bed electrode cell was 20–30% higher than that in the flooded packed-bed electrode cell.

Nomenclature

A_b resistance coefficient for bypass current (m^{-1})
A_s resistance coefficient for total current flowing through spacer region (m^{-1})
C_C concentration of Na_2SO_4 ($mol\,m^{-3}$)
C_e overall current efficiency
C_i concentration of Cu^{2+} in ith cell, function of time ($mol\,m^{-3}$)
C_0 concentration of Cu^{2+} in reservoir, function of time ($mol\,m^{-3}$)
$C_0(0)$ initial value of C_0 ($mol\,m^{-3}$)
d diameter of pellet (m)
D diffusion coefficient ($m^2\,s^{-1}$)
e_i potential difference between upper and lower ends of each pellet (V)
E cell voltage (V)
F Faraday constant ($C\,mol^{-1}$)
I_b mean value of I_{bi} (A)
I_{bi} bypass current in ith cell, function of time (A)
I_p mean value of I_p (A)
I_{pi} faradaic current in ith cell, function of time (A)
I_t total current (A)
k mass transfer coefficient ($m\,s^{-1}$)
L_T distance between two feeder electrodes (m)
n number of pellet layers
Q volumetric flow rate of electrolyte ($m^3\,s^{-1}$)
R_{bi} equivalent resistance for bypass current in ith cell, function of time (Ω)
R_{pi} equivalent resistance for faradaic current in ith cell, function of time (Ω)
R_{si} equivalent resistance for total current in ith cell, function of time (Ω)
Re_d Reynolds number, du_l/v_l
Sc Schmidt number, v_l/D
Sh_d Sherwood number, kd/D
S_p total surface area of cathodic part of bipolarized pellets in each layer, defined by Equation 9 (m^2)
S_T cross-sectional area of column (m^2)
t time (s)

0021–891X/87 $03.00 + .12

u_l superficial liquid velocity ($m\,s^{-1}$)
V_r volume of reservoir (m^3)
z number of electrons transferred in electrochemical reaction
ε_l liquid holdup
κ mean value of κ_i ($S\,m^{-1}$)
κ_i electrical conductivity of electrolyte in ith cell, function of time ($S\,m^{-1}$)
$\kappa(0)$ initial value of κ ($S\,m^{-1}$)
λ molar conductivity ($S\,mol^{-1}\,m^{-2}$)
ν_l kinematic viscosity ($m^2\,s^{-1}$)

Subscripts
A $CuSO_4$
B H_2SO_4
C Na_2SO_4

1. Introduction

Bipolar particle electrode cells consist of electrically conductive particles which are packed [1–12] or fluidized [13] between feeder electrodes. Particles have to be insulated from adjacent ones by dilution with non-conducting particles [2] or by spacers [6–12]. When a sufficiently steep potential drop is applied across the bed, one side of each particle becomes cathodic and the other side anodic. These cells have been applied to water treatment [1, 4, 5, 10–12] and electroorganic synthesis [2, 3, 6, 7, 13] processes where the liquid conductivity and the current density are not high.

Current pathways flowing in bipolar packed-bed electrode cells were analysed on the basis of equivalent resistance models [4–6, 14]. Kusakabe *et al.* [4–6] carried out the reduction of Cu(II) ions and determined the effects of particle diameter, cell voltage, packing mode and electrolyte compositions on the overall current efficiency. Their results indicate that overall current efficiency increases with increasing faradaic current (current passing through particles) compared to total current and also with decreasing conductivity of electrolyte.

Fleischmann *et al.* [2] analysed the concentration at the cell outlet assuming a plug flow of electrolyte in a packed-bed cell. Ehadaie *et al.* [10] further considered the potential distribution across bipolarized particles in a trickle-bed cell.

When a bipolar packed-bed cell is used to remove heavy metal ions from waste water, the liquid is usually recirculated through the cell. In this case, concentration of reactants, liquid conductivity and pH values vary with time, which consequently causes changes in the faradaic current and the current efficiency. Therefore, unsteady-state simulation of the bipolar packed-bed is essential for practical operations.

In this study, unsteady-state characteristics of a bipolar packed-bed electrode cell are investigated by using the electroremoval of copper from copper sulphate solutions. Total current, faradaic current, liquid conductivity and overall current efficiency are measured with time elapsed, and are analysed by a reactor model. The overall current efficiency of a bipolar trickle-bed cell is also measured in comparison with the bipolar packed-bed cell.

2. Experimental details

Fig. 1 shows a schematic diagram of a bipolar packed-bed or trickle-bed electrode cell. The cell was made of transparent PMMA plastic pipe, 6.6 cm in diameter and 20 cm in total height. The feeder electrodes were perforated plates (hole diameter = 3 mm, fractional free area = 23%) and were made of graphite plate for the anode and of platinum-coated titanium plate for the cathode. The platinum-coated titanium plate was used so that the initial condition of the

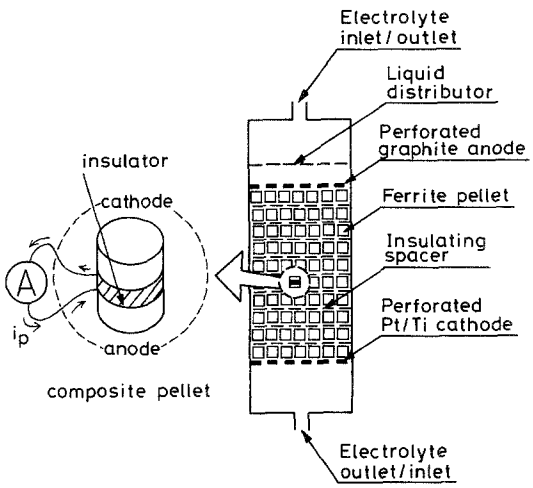

Fig. 1. Schematic diagram of bipolar packed-bed or trickle-bed electrode cell.

cathodic feeder might be recovered after washing with a dilute HNO_3 solution. These feeders were fixed 10.5 cm apart vertically. A perforated plastic plate (hole diameter = 1 mm, fractional free area = 0.78%) was fixed 2 cm above the anode and was used as the liquid distributor in the case of trickle-flow operation. Cylindrical sintered ferrite pellets ($NiFe_2O_4$) were packed between the two feeders. Each pellet was 4 or 6 mm in diameter and 4 or 6 mm long, respectively. Polyethylene net, 1 mm thick, was inserted between the pellet layers in parallel with the feeder electrodes, and divided the packed bed into 21 (for 4 mm pellets) or 15 (for 6 mm pellets) layers of pellets. About 231 (for 4 mm) or 85 (for 6 mm) pellets were packed at random in each layer. Some pellets in each layer stood vertically and others lay on their sides. The plastic net was also inserted between feeder electrodes and adjacent pellet layers.

The electrolyte phase was a copper sulphate solution of 10 mol m^{-3}. To adjust the conductivity, sodium sulphate was dissolved in the solution. The conductivity of the electrolyte was measured by means of a Kohlrausch bridge. The electrolyte was kept at 298 K in a reservoir with a capacity of 2 litres. When the bed was operated in the flooded flow mode, the electrolyte was introduced upward at a superficial velocity of 0.97 cm s^{-1}. In the case of trickle flow, however, the electrolyte flowed downward at 0.49 cm s^{-1}.

Electrolysis was conducted at constant voltage. The amount of electricity passed was measured by means of a coulometer. Total current and liquid conductivity were continuously recorded. The faradaic current was measured by using monitor electrodes [5, 6] embedded at five positions in the column. The monitor electrodes, shown in Fig. 1, were prepared as follows. A pellet was cut into halves and a thin paper was sandwiched between them as an insulator. A lead wire was pasted to the inside plane of each half to measure the electric current flowing in the pellet. The size of the monitor electrodes was the same as the original pellets.

The electrolyte was sampled regularly, and the copper concentration was analysed by potentiometry with EDTA. The bypass current was measured by packing with inert glass pellets which were identical to the ferrite pellets in shape. The bypass current was also determined by subtracting the faradaic current from the total current. The values obtained by both methods coincided well.

The polarization curve for the cathodic deposition of copper was measured with a single pellet electrode which was set in the bed of glass pellets. The working pellet electrode was insulated with epoxy resin except for the plane facing the feeder. The potential of the working electrode was measured using a Luggin capillary which was connected to a saturated Ag/AgCl reference electrode.

3. Reactor model with recirculating feed

Fig. 2 shows the equivalent resistance model of a bipolar packed-bed electrode cell. The electrode reactions are expressed by

Anode:

$$H_2O \longrightarrow 2H^+ + \tfrac{1}{2}O_2 + 2e \qquad (1)$$

Cathode:

$$Cu^{2+} + 2e \longrightarrow Cu \qquad (2)$$

As shown in Fig. 2, the total current flowing through the free space of the insulation nets is described by

$$I_t = I_{pi} + I_{bi} \qquad (3)$$

The equivalent resistance for the bypass current and the total current are reciprocally proportional to the liquid conductivity.

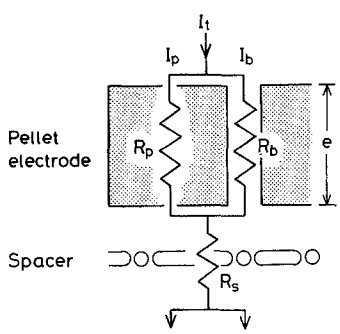

Fig. 2. Equivalent resistance model for current pathways in bipolar packed-bed or trickle-bed electrode cell.

$$R_{bi} = A_b/\kappa_i \quad (4)$$

$$R_{si} = A_s/\kappa_i \quad (5)$$

where A_b and A_s are resistance coefficients which depend on the geometry and the arrangement of packings.

The potential difference along the vertical length of each pellet is equal to the ohmic drop in the bypass region. To simplify the calculation, it is assumed that e_i is constant for every unit cell of pellets layer and is only a function of time. Therefore,

$$e = I_{bi}R_{bi}$$

$$= (I_t - I_{pi})A_b/\kappa_i \simeq (I_t - I_p)A_b/\kappa \quad (6)$$

By assuming that the feeder electrodes functioned as an additional pellet layer, the total cell voltage is given as

$$E = (n + 1)(e + I_t R_{si}) \quad (7)$$

Then the faradaic current in the ith cell is given by

$$I_{pi} = zFkS_pC_i \quad (8)$$

where it is assumed that the cathodic reaction is completely controlled by the diffusion of Cu(II) ions, and also that the intrinsic current efficiency is unity. The total cathode area in each pellet layer is defined by

$$S_p = (\text{number of pellets in each layer}) \times (\text{mean copper deposited area of each layer}) \quad (9)$$

The ratio of the mean copper deposited area of each pellet to the surface area of a pellet was determined as 0.40 from the previous study [5].

From Equations 6, 7 and 8, the bypass current is expressed by

$$I_{bi} = \kappa_i E/[(A_b + A_s)(n + 1)] - [A_s/(A_b + A_s)]zFkS_pC_i \quad (10)$$

Fig. 3 shows the reactor model for the recirculating feed operation. If each pellet layer behaves as a back-mix type reactor, the material balance in the ith cell is given as

$$Q(C_{i-1} - C_i) = I_{pi}/(zF) \quad (11)$$

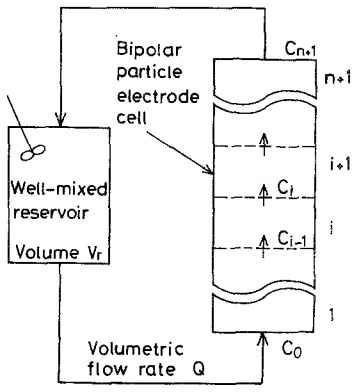

Fig. 3. Reactor model with recirculating feed.

From Equations 8 and 11,

$$C_i = C_{i-1}/(1 + kS_p/Q) = C_0/(1 + kS_p/Q)^i \quad (12)$$

The material balance in the reservoir is

$$V_r dC_0/dt = Q(C_{n+1} - C_0) \quad (13)$$

By combining Equations 12 and 13,

$$V_r dC_0/dt = -QC_0[1 - (1 + kS_p/Q)^{-(n+1)}] \quad (14)$$

Integrating Equation 14 gives

$$C_0 = C_0(0) \times \exp\{-t/(V_r/Q)[1 - (1 + kS_p/Q)^{-(n+1)}]\} \quad (15)$$

Then the concentration in the ith cell is given as

$$C_i = C_0(0)/(1 + kS_p/Q)^i \times \exp\{-t/(V_r/Q)[1 - (1 + kS_p/Q)^{-(n+1)}]\} \quad (16)$$

The liquid conductivity is affected by the concentrations of $CuSO_4$, Na_2SO_4 and H_2SO_4 and is given as follows:

$$\kappa_i = \lambda_A C_i + \lambda_B[C_i(0) - C_i] + \lambda_C C_C \quad (17)$$

where C_i is expressed by Equation 16, and λ_A, λ_B and λ_C are the molar conductivities of $CuSO_4$, H_2SO_4 and Na_2SO_4, respectively. The molar conductivity of H_2SO_4 is a function of the dissociation condition.

4. Experimental results and discussion

4.1. *Bipolar packed-bed electrode*

4.1.1. Change in copper concentration. Fig. 4 shows the change in copper concentration with time elapsed. The copper concentration does not fall much below $0.5\,\mathrm{mol\,m^{-3}}$. This is probably due to re-dissolution of deposited copper. The only unknown parameter, i.e. the mass transfer coefficient, k, in Equation 15 was determined by using the non-linear least squares method in the range of $C_0 = 1$–$10\,\mathrm{mol\,m^{-3}}$. The solid lines in Fig. 4 are calculated from Equation 15 with most probable values of k.

Fig. 5 shows the effect of liquid conductivity on the mass transfer coefficient, which is nearly constant in the range $\kappa(0) > 0.8\,\mathrm{S\,m^{-1}}$. The black circle is the mass transfer coefficient obtained experimentally from the polarization curve. The broken line is estimated from the following equation [15] which can be applied in the range of Reynolds number 0.0016–55,

$$Sh_d = (1.09/\varepsilon_l) Re_d^{1/3} Sc^{1/3} \qquad (18)$$

The data obtained at higher electrolyte conductivities agree with Equation 18. The reaction rate is controlled by the mass transfer of copper ions in this region.

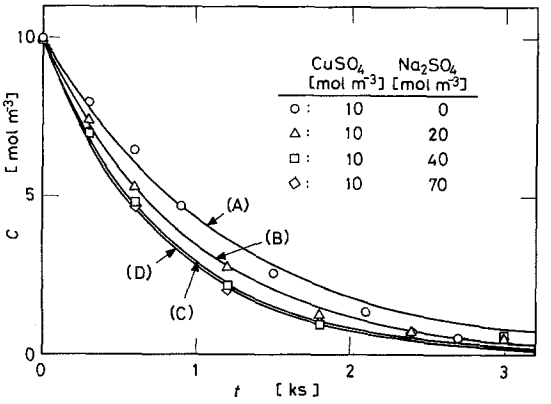

Fig. 4. Change in copper concentration in bipolar packed-bed electrode cell, with 21 layers of 4 mm pellets, cell voltage = 50 V. Values of k: (A) $1.76 \times 10^{-5}\,\mathrm{m\,s^{-1}}$; (B) $2.22 \times 10^{-5}\,\mathrm{m\,s^{-1}}$; (C) $2.62 \times 10^{-5}\,\mathrm{m\,s^{-1}}$; (D) $2.70 \times 10^{-5}\,\mathrm{m\,s^{-1}}$.

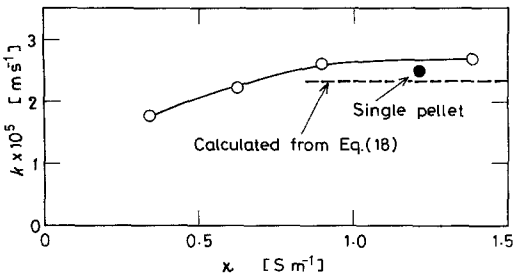

Fig. 5. Effect of liquid conductivity on mass transfer coefficient on the cathodic side of each pellet in bipolar packed-bed electrode cell, with 21 layers of 4 mm pellets, electrolyte = $10\,\mathrm{mol\,m^{-3}}$ $CuSO_4$, at 298 K. ●, from polarization curve; – – –, from Equation 18.

4.1.2. Change in current. Fig. 6 shows the changes in the total current, the faradaic current and the bypass current with time. The initial composition of the electrolyte is $10\,\mathrm{mol\,m^{-3}}$ $CuSO_4$ + $70\,\mathrm{mol\,m^{-3}}$ Na_2SO_4. Fig. 7 illustrates the changes in the total current and the bypass current without the addition of Na_2SO_4. The line (C) in Figs 6 and 7 indicates the average value of I_{pi} calculated from Equations 8 and 16. The production of sulphuric acid by Reaction 1 increases the liquid conductivity and consequently the bypass current which is expressed by

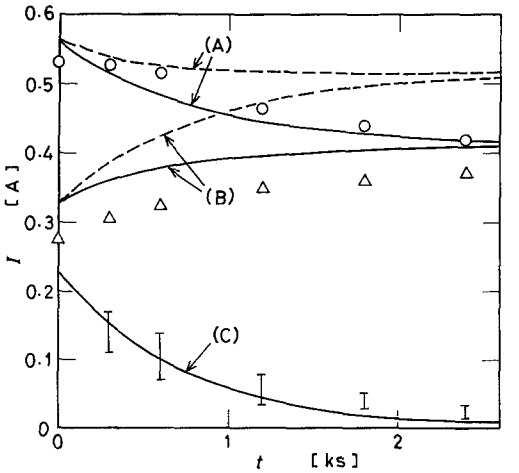

Fig. 6. Changes in currents in bipolar packed-bed electrode cell, with 21 layers of 4 mm pellets, electrolyte = $10\,\mathrm{mol\,m^{-3}}$ $CuSO_4$ + $70\,\mathrm{mol\,m^{-3}}$ Na_2SO_4, cell voltage = 45 V. ○ and (A), Total current; △ and (B), bypass current; I and (C), faradaic current. The solid line is calculated with limiting molar conductivity of H^+ and HSO_4^-, the broken line is calculated with molar conductivity of H_2SO_4.

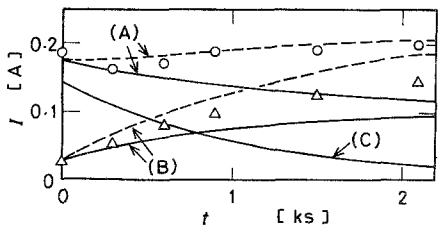

Fig. 7. Changes in currents in bipolar packed-bed electrode cell, with 21 layers of 4 mm pellets, electrolyte = 10 mol m^{-3} $CuSO_4$, cell voltage = 50 V. ○ and (A), Total current; △ and (B), bypass current; (C), faradaic current. The solid line is calculated with limiting molar conductivity of H^+ and HSO_4^-, the broken line is calculated with molar conductivity of H_2SO_4.

Equation 10. The resistance coefficient for the total current was estimated as $A_s = 0.83\,m^{-1}$ from the previous experiment [6] by correcting the cross-sectional area of the bed. This value was substituted for A_s in the following Bruggeman equation [16], and the resistance coefficient for the bypass current was obtained as $A_b = 7.60\,m^{-1}$.

$$nA_b + (n + 1)A_s = \varepsilon_l^{-1.5} L_T/S_T \quad (19)$$

The solid and broken lines (B) in Figs 6 and 7 indicate the average value of I_{bi} calculated from Equations 10, 16 and 17. The data for the bypass current plotted in Figs 6 and 7 were calculated from Equation 10 by using the experimental values of conductivity and Cu^{2+} concentration of the electrolyte. The broken line (B) was calculated by using Equation 17 where the liquid conductivity was estimated from the molar conductivities of $CuSO_4$, Na_2SO_4 and H_2SO_4. The difference between the data expressed by the triangular symbol and the calculated line (B) is mainly caused by the error in the estimation of liquid conductivity. The effect of co-existing components on the ion equilibrium is not considered in this case.

On the other hand, the solid line (B) is calculated from Equation 17 with the limiting molar conductivities of H^+ and HSO_4^-. When Na_2SO_4 is dissolved in the electrolyte, most of the H_2SO_4 dissociates into $H^+ + HSO_4^-$ [17]. Thus the experimental bypass current is well expressed by the solid line (B) as shown in Fig. 6. Without the addition of Na_2SO_4, however, the experimental values of I_b lie between the solid and broken lines (B) as shown in Fig. 7.

Fig. 8 shows the change in the overall current efficiency averaged over the electrolysis period t. The overall current efficiency decreases with increasing liquid conductivity and with decreasing copper ion concentration and is given by

$$C_e = \Delta C z F V_r \Big/ \int I_t\,dt = \left[(n + 1)\int I_p\,dt + \int I_b\,dt\right] \Big/ \int I_t\,dt \quad (20)$$

The overall current efficiency per unit pellet layer is about 0.70 at maximum under the present conditions.

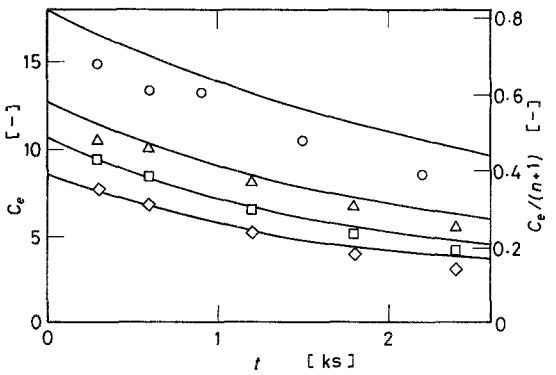

Fig. 8. Change in overall current efficiency, with 21 layers of 4 mm pellets, cell voltage = 50 V. ○, 10 mol m^{-3} $CuSO_4$; △, 10 mol m^{-3} $CuSO_4$ + 20 mol m^{-3} Na_2SO_4; □, 10 mol m^{-3} $CuSO_4$ + 40 mol m^{-3} Na_2SO_4; ◇, 10 mol m^{-3} $CuSO_4$ + 70 mol m^{-3} Na_2SO_4. The solid lines are calculated from Equations 8, 10 and 20.

4.2. *Bipolar trickle-bed electrode*

As shown in Fig. 8, a decrease in the overall current efficiency is unavoidable in recirculating operation. Therefore, the bypass current must be minimized by decreasing the liquid hold-up in the bed. In the previous paper [5], the introduction of gas bubbles from the bottom of the bed improved the overall current efficiency by 60%. In this study trickle flow was tested.

Fig. 9 shows the total current versus cell voltage curves in the trickle-bed electrode cell. The broken lines indicate the bypass current measured with inert pellets. The faradaic current in the trickle-bed electrode cell was about 70% of that

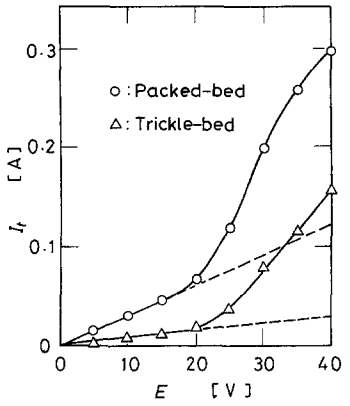

Fig. 9. Total current versus cell voltage curves in bipolar packed-bed and trickle-bed electrode cells, with 15 layers of 6 mm pellets, electrolyte = 10 mol m^{-3} $CuSO_4$ + 20 mol m^{-3} Na_2SO_4.

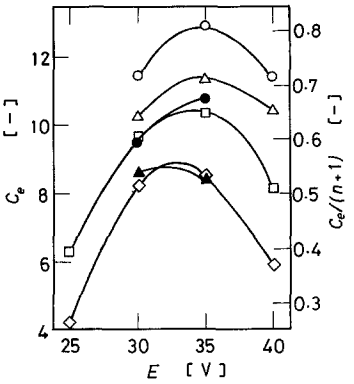

Fig. 10. Overall current efficiency in bipolar packed-bed and trickle-bed electrode, with 15 layers of 6 mm pellets. ○, Trickle-bed, 10 mol m^{-3} $CuSO_4$; ●, packed-bed, 10 mol m^{-3} $CuSO_4$; △, trickle-bed, 10 mol m^{-3} $CuSO_4$ + 20 mol m^{-3} Na_2SO_4; ▲, packed-bed, 10 mol m^{-3} $CuSO_4$ + 20 mol m^{-3} Na_2SO_4; □, trickle-bed, 10 mol m^{-3} $CuSO_4$ + 40 mol m^{-3} Na_2SO_4; ◇, trickle-bed, 10 mol m^{-3} $CuSO_4$ + 70 mol m^{-3} Na_2SO_4.

in the packed-bed cell. However, the bypass current was about a quarter that of the packed-bed cell.

Fig. 10 indicates the relationship between the cell voltage and the overall current efficiency averaged over the initial 10 min. The overall current efficiency in the trickle-bed cell is increased by 20–30% compared with the packed-bed cell. The biggest overall current efficiency per unit pellet layer in the trickle-bed cell is 0.80. The optimum cell voltage appears, because at lower voltages only a fraction of the available area on the pellets is rendered bipolar and at higher voltages hydrogen is evolved.

5. Conclusions

Unsteady state changes in faradaic current and bypass current in a bipolar packed-bed electrode cell were analysed using the model shown in Fig. 3. The currents through different pathways were simplified as in Fig. 2. The faradaic current decreased with decreasing copper ion concentration as the reaction proceeded. The bypass current increased with increasing liquid conductivity due to the production of hydrogen ions. Thus, the decrease of overall current efficiency was unavoidable in the recirculating operation.

The overall current efficiency in the trickle-bed cell was increased by 20–30% in comparison with the flooded packed-bed cell.

References

[1] A. B. Smith and M. J. Hayes, Ger. Offen. 1949129, 9 April (1970).
[2] M. Fleischmann, J. W. Oldfield and C. L. K. Tennakoon, Symposium on Electrochemical Engineering, University of Newcastle-upon-Tyne, Vol. I (1971) p. 53.
[3] F. Goodridge, C. J. H. King and A. R. Wright, *Electrochim. Acta* **22** (1977) 347.
[4] K. Kusakabe, S. Morooka and Y. Kato, *J. Chem. Eng. Japan* **15** (1982) 45.
[5] K. Kusakabe, T. Kimura, S. Morooka and Y. Kato, *ibid.* **17** (1984) 293.
[6] K. Kusakabe, S. Morooka and Y. Kato, *ibid.* **19** (1986) 43.
[7] A. V. Boussoulengas, S. Ehdaie and R. E. W. Jansson, *Chem. and Ind.* Oct. (1979) 670.
[8] M. Fleischmann and Z. Ibrisagic, *J. Appl. Electrochem.* **10** (1980) 151.
[9] K. G. Ellis and R. E. W. Jansson, *ibid.* **11** (1981) 531.
[10] S. Ehadaie, M. Fleischmann and R. E. W. Jansson, *ibid.* **12** (1982) 59.
[11] E. A. El-Ghaoui, R. E. W. Jansson and A. R. Wright, *ibid.* **12** (1982) 69.
[12] E. A. El-Ghaoui and R. E. W. Jansson, *ibid.* **12** (1982) 75.
[13] F. Goodridge, C. J. H. King and A. R. Wright, *Electrochim. Acta* **22** (1977) 1087.
[14] C. J. H. King, K. Lister and R. E. Plimley, *Trans. Instn Chem. Engrs* **53** (1977) 20.
[15] E. J. Wilson and C. J. Geankoplis, *Ind. Eng. Chem. Fundam.* **5** (1966) 9.
[16] D. A. G. Bruggeman, *Ann. Phisik.* **24** (1935) 636.
[17] J. Newman, 'Electrochemical Systems', Prentice Hall (1973) p. 364.